A NONCONFORMING IMMERSED FINITE ELEMENT METHOD FOR ELLIPTIC INTERFACE PROBLEMS

TAO LIN†, DONGWOO SHEEN‡, AND XU ZHANG§

Abstract. A new immersed finite element (IFE) method is developed for second-order elliptic problems with discontinuous diffusion coefficient. The IFE space is constructed based on the rotated-Q_1 nonconforming finite elements with the integral-value degrees of freedom. The standard nonconforming Galerkin method is employed in this IFE method without any stabilization term. Error estimates in energy and L^2-norms are proved to be better than $O(h\sqrt{|\log h|})$ and $O(h^2|\log h|)$, respectively, where the $|\log h|$ factors reflect jump discontinuity. Numerical results are reported to confirm our analysis.

Key words. immersed finite element, nonconforming, rotated-Q_1, Cartesian mesh, elliptic interface problem

AMS subject classifications. 35R05, 65N15, 65N30

1. Introduction.

We consider the second-order elliptic interface problem:

$$-\nabla\cdot(\beta\nabla u) = f \quad \text{in } \Omega^-\cup\Omega^+, \tag{1.1a}$$

$$u = g \quad \text{on } \partial\Omega, \tag{1.1b}$$

where, without loss of generality, we assume that a C^2-continuous interface curve Γ separates the physical domain Ω into two sub-domains Ω^- and Ω^+, such that $\overline{\Omega}=\overline{\Omega^+}\cup\overline{\Omega^-}\cup\Gamma$, see an illustration in Figure 1.1. The physical domain $\Omega\subset\mathbb{R}^2$ is assumed to be occupied by two materials such that the diffusion coefficient $\beta(x,y)$ is discontinuous across the interface Γ, and it is assumed to be a piecewise constant function defined by

$$\beta(x,y)=\begin{cases}\beta^- & \text{if } (x,y)\in\Omega^-,\\ \beta^+ & \text{if } (x,y)\in\Omega^+,\end{cases} \tag{1.2}$$

such that $\min\{\beta^-,\beta^+\}>0$. Across the interface Γ, the solution and the normal component of the flux are assumed to be continuous, *i.e.*,

$$[u]_\Gamma = 0, \tag{1.3a}$$

$$[\![\boldsymbol{\nu}\cdot\beta\nabla u]\!]_\Gamma = 0, \tag{1.3b}$$

where $[v]_\Gamma=v^+|_\Gamma-v^-|_\Gamma$, and $[\![\boldsymbol{\nu}\cdot\beta\nabla u]\!]_\Gamma=\boldsymbol{\nu}^+\cdot\beta^+\nabla u^+ + \boldsymbol{\nu}^-\cdot\beta^-\nabla u^-$, with $\boldsymbol{\nu}$ the unit normal of Γ.

Conventional finite element methods (FEM) can solve this elliptic interface problem satisfactorily provided that solution meshes are shaped to fit the material interface [5]; otherwise the accuracy of the solution is uncertain [1, 14]. *Immersed finite element* (IFE) methods [3, 10, 13, 15, 20, 24, 25, 29, 30, 32], on the other hand, do not

*This research was partially supported by the National Science Foundation Grant (DMS-1016313, DMS-1720425), NRF–2017R1A2B3012506 and NRF-2015M3C4A7065662 in part.

†Department of Mathematics, Virginia Tech, Blacksburg, VA 24061, tlin@math.vt.edu

‡Department of Mathematics, and Interdisciplinary Program in Computational Science & Technology, Seoul National University, Seoul 08826, Korea, dongwoosheen@gmail.com

§Department of Mathematics and Statistics, Mississippi State University, Mississippi State, MS 39762, xuzhang@math.msstate.edu

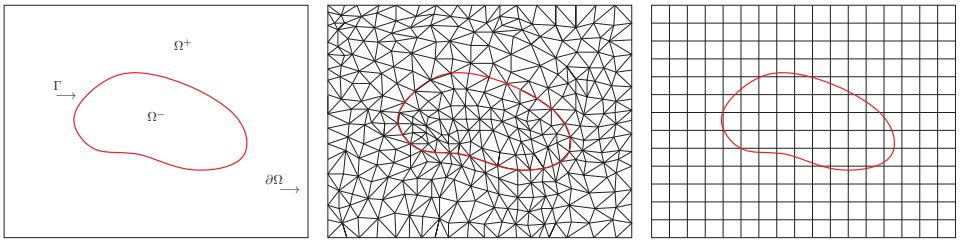

FIG. 1.1. *Body-fitting mesh and non-body-fitting mesh of an interface problem*

require meshes to fit the interface. Hence, if desired, Cartesian meshes can be used to solve interface problems which is advantageous in many simulations. For example, in particle-in-cell methods for plasma-particle simulations [21, 22], it is preferable to solve the governing electric potential equation on Cartesian meshes for efficient particle tracking. Also, IFE methods, in either a standard fully discrete or a semi-discrete (method of lines) formulation, can be used to solve time-dependent problems with moving interfaces [19, 27] on a fixed Cartesian mesh throughout the whole simulation.

The basic idea of IFE methods is to locally modify finite element functions on interface elements to fit the interface jump conditions (1.3a) and (1.3b). For elliptic interface problems, most IFE methods in the literature are modified from the Lagrange-type finite element spaces (usually H^1-conforming), whose degrees of freedom are determined by nodal values at the mesh points. However, IFE spaces originated from these conforming FE spaces are usually nonconforming because IFE functions are discontinuous across interface edges. This discontinuity can be harmfully large for certain configuration of interface locations and diffusion coefficients. Consequently, the IFE solution is often less accurate around the interface than the rest of solution domain. Our recent study in [28, 33] indicates that the convergence rates of these Lagrange-type IFE functions used in the Galerkin formulation can sometimes deteriorate as the mesh size gets small. In [28], a partially penalized immersed finite element (PPIFE) method was developed to cope with the discontinuity of Lagrange-type IFE functions. The PPIFE method is shown to converge optimally in the energy norm.

Another framework to construct the IFE approximation is based on nonconforming finite elements [4, 7, 23, 31]. One significant difference between conforming and nonconforming finite elements is the way to impose the continuity of finite element functions across elements. Conforming FE enforces the continuity through nodal values at mesh points, while the continuity of nonconforming FE is usually weakly imposed through mean values over edges/faces. The simplest nonconforming finite element defined on simplicial meshes is the well-known Crouzeix-Raviart (CR) element [7]. For rectangular meshes, the simplest nonconforming finite elements are known as the *rotated-*Q_1 finite elements [4, 23, 31].

In this article, we develop and analyze an IFE method based on the nonconforming rotated-Q_1 FEM without any stabilization term. Our error estimates show that the method converges optimally sans factors of $|\log(h)|$ in both energy and L^2-norms with standard piecewise H^2-regularity assumption. The main technique in our error analysis is based on a special projection operator introduced in [8] to bound the flux error on edges. We extend this projection to interface problems and show that

the error bound of flux on interface edges induces a $|\log(h)|$ factor, which is crucial for piecewise smooth functions, and therefore unremovable for interface problems. The analytical technique in our error estimation is new to interface problems. Also, the proposed IFE method here can be readily extended for solving problems with nonhomogeneous jump conditions across the interface by following a homogenization technique such as those developed in [10, 17].

The rest of this article is organized as follows. In Section 2, we construct the nonconforming rotated-Q_1 IFE space and present some basic properties. In Section 3, we discuss the approximation capabilities of the IFE space. In Section 4, we analyze the error bounds of Galerkin IFE approximation to the elliptic interface problem in energy and L^2-norms. In Section 5, numerical results are presented to confirm our analysis and to demonstrate features of the new IFE method. Finally, a few brief conclusions are provided in Section 6.

2. Nonconforming Immersed Finite Element Space. This section starts with notations and some preliminaries to be used in this paper. Then, we will introduce the IFE space based on nonconforming rotated-Q_1 elements.

2.1. Notations and Preliminaries. Multi-index notations will be employed such that $\alpha = (\alpha_1, \alpha_2) \in [\mathbb{Z}^+]^2, |\alpha| = \alpha_1 + \alpha_2$, together with the partial differential operator $\partial^\alpha = \frac{\partial^{\alpha_1}}{\partial x_1^{\alpha_1}} \frac{\partial^{\alpha_2}}{\partial x_2^{\alpha_2}}$, where $\mathbb{Z}^+$ denotes the set of all nonnegative integers.

Let $S \subseteq \Omega$ be an open set such that $S \cap \Gamma \neq \emptyset$, and let $S^s = S \cap \Omega^s, s = -, +$. Then, let $\widetilde{S} = S^- \cup S^+$ and we note that $\widetilde{S} \neq S$. Let $W^{m,p}(\widetilde{S})$ denote the usual Sobolev space on the open set $\widetilde{S}$ with non-negative integer index m, equipped with the norm and seminorm:

$$\|v\|_{W^{m,p}(\widetilde{S})} = \Big(\sum_{|\alpha| \leq m} \int_{\widetilde{S}} |\partial^\alpha v(\mathbf{x})|^p \, \mathrm{d}\mathbf{x} \Big)^{1/p}, \quad |v|_{W^{m,p}(\widetilde{S})} = \Big(\sum_{|\alpha| = m} \int_{\widetilde{S}} |\partial^\alpha v(\mathbf{x})|^p \, \mathrm{d}\mathbf{x} \Big)^{1/p},$$

for $1 \leq p < \infty$, and

$$\|v\|_{W^{m,\infty}(\widetilde{S})} = \max_{|\alpha| \leq m} \operatorname*{ess.sup}_{\mathbf{x} \in \widetilde{S}} |\partial^\alpha v(\mathbf{x})|, \quad |v|_{W^{m,\infty}(\widetilde{S})} = \max_{|\alpha| = m} \operatorname*{ess.sup}_{\mathbf{x} \in \widetilde{S}} |\partial^\alpha v(\mathbf{x})|.$$

In particular, for $p = 2$, we denote $H^m(\widetilde{S}) = W^{m,p}(\widetilde{S})$, and we omit the index p in associated norms and seminorms for simplicity, *i.e.*, $\|v\|_{W^{m,2}(\widetilde{S})} = \|v\|_{H^m(\widetilde{S})}$, and $|v|_{W^{m,2}(\widetilde{S})} = |v|_{H^m(\widetilde{S})}$. We will also follow the convention to drop the domain index $\widetilde{S}$ if $\widetilde{S} = \widetilde{\Omega}$. For $p = 2$, associated with the norm $\|\cdot\|_{H^m(\widetilde{S})}$, the inner product for $H^m(\widetilde{S})$ will be denoted by $(\cdot,\cdot)_{H^m(\widetilde{S})}$, with further simplification to $(\cdot,\cdot)_{\widetilde{S}}$ and $(\cdot,\cdot)$ if $m = 0$ and also if $\widetilde{S} = \widetilde{\Omega}$, respectively.

For $m \geq 1$, we define two types of subspaces of $H^m(\widetilde{S})$ whose functions satisfy the interface jump conditions (1.3a) and (1.3b) on Γ. First, we set

$$\widetilde{H}^m_\Gamma(S) = H^1(S) \cap H^m(\widetilde{S}),$$

endowed with the inner-product and the norm

$$\langle u, v \rangle_{\widetilde{H}^m(S)} = (u, v)_{H^1(S)} + \sum_{s=-,+} \sum_{|\boldsymbol{\alpha}|=2}^{m} (\partial^{\boldsymbol{\alpha}} u, \partial^{\boldsymbol{\alpha}} v)_{L^2(S^s)}, \quad \|u\|_{\widetilde{H}^m(S)} = \sqrt{\langle u, u \rangle_{\widetilde{H}^m(S)}}.$$

Notice that $\widetilde{H}^1_\Gamma(S) = H^1(S)$ and that

$$[v]_{\Gamma\cap S} = 0 \text{ in the sense of } H^{\frac{1}{2}}(\Gamma\cap S) \quad \forall v \in \widetilde{H}^m_\Gamma(S),\ m \geq 1.$$

In addition, for $m = 2$, we define a subspace of $\widetilde{H}^m_\Gamma(S)$ as follows:

$$\widetilde{H}^2_\beta(S) = \left\{ v \in \widetilde{H}^2_\Gamma(S) :\ [\![\boldsymbol{\nu}_\Gamma \cdot \beta\nabla v]\!]_{\Gamma\cap S} = 0 \right\}$$

where the jump of the flux is understood in the sense of $H^{\frac{1}{2}}(\Gamma)$. Furthermore, the concepts above can be readily extended to define the following spaces and the related norms: for $p > 2$,

$$\widetilde{W}^{2,p}_\Gamma(S) = W^{1,p}(S) \cap W^{2,p}(\widetilde{S}), \quad \widetilde{W}^{2,p}_\beta(S) = \{v \in \widetilde{W}^{2,p}_\Gamma(S) \mid\ [\![\boldsymbol{\nu}_\Gamma \cdot \beta\nabla v]\!]_{\Gamma\cap S} = 0\}.$$

Assume that $f \in H^{-1}(\Omega)$, where $H^{-1}(\Omega)$ is the dual space of $H^1_0(\Omega) = \widetilde{H}^1_{\Gamma,0}(\widetilde{\Omega})$. For the interface problem described by (1.1) and (1.3), we consider its weak form: find $u \in H^1(\Omega)$ such that $u = g$ on $\partial\Omega$ and

$$a(u, v) = L(v) \quad \forall\ v \in H^1_0(\Omega), \tag{2.1}$$

where

$$a(u, v) = (\beta\nabla u, \nabla v), \quad L(v) = \langle f, v\rangle_{H^{-1}(\Omega), H^1_0(\Omega)},$$

$\langle\cdot,\cdot\rangle_{V',V}$ being the duality pairing between the topological vector space V and its dual space V'. An application of the Lax-Milgram Lemma shows that there exists a unique solution $u \in H^1(\Omega)$ for (2.1) such that

$$\|u\|_{H^1(\Omega)} \leq C\|f\|_{H^{-1}(\Omega)},$$

where C is a positive constant depending only on Ω and β.

2.2. Nonconforming FE functions. Let Ω be a rectangular domain or a union of rectangular domains. Without loss of generality, assume that $\{\mathcal{T}_h\}$ is a family of uniform Cartesian meshes for domain Ω with mesh parameter $h > 0$. For each element $T \in \mathcal{T}_h$, we call it an interface element if the interior of T intersects with the interface Γ; otherwise, we call it a non-interface element. Without loss of generality, we assume that interface elements in $\mathcal{T}_h$ satisfy the following hypotheses when the mesh size h is small enough:

(H1). The interface Γ cannot intersect an edge of any element at more than two points unless the edge is part of Γ.

(H2). If Γ intersects the boundary of an element at two points, these intersection points must be on different edges of this element.

(H3). The interface Γ is a piecewise C^2-continuous function, and the mesh $\mathcal{T}_h$ is formed such that the subset of Γ in every interface element is C^2-continuous.

Denote by $\mathcal{T}_h^I$ and $\mathcal{T}_h^N = \mathcal{T}_h \setminus \mathcal{T}_h^I$ the collections of all interface elements and non-interface elements, respectively. For a typical rectangular element $T = \square A_1A_2A_3A_4 \in \mathcal{T}_h$, the following conventions for its vertices and edges are assumed:

$$A_1 = (x_0, y_0),\quad A_2 = (x_0 + h_x, y_0),\quad A_3 = (x_0 + h_x, y_0 + h_y),\quad A_4(x_0, y_0 + h_y), \tag{2.2}$$

and

$$\gamma_1 = \overline{A_1A_2},\quad \gamma_2 = \overline{A_2A_3},\quad \gamma_3 = \overline{A_3A_4},\quad \gamma_4 = \overline{A_4A_1}. \tag{2.3}$$

We follow the classical triplet definition of a finite element [6]. On the element T, the local FE space is defined by

$$\Pi_T = \text{Span}\left\{1, \frac{x-x_0}{h_x}, \frac{y-y_0}{h_y}, \left(\frac{x-x_0}{h_x}\right)^2 - \left(\frac{y-y_0}{h_y}\right)^2\right\}. \tag{2.4}$$

The degrees of freedom are defined as the mean values over edges:

$$\Sigma_T = \left\{\frac{1}{|\gamma_j|}\int_{\gamma_j} \psi_T \, \mathrm{d}s, j = 1,2,3,4 : \forall\ \psi_T \in \Pi_T\right\}, \tag{2.5}$$

where $|\gamma_j|$ denotes the length of the edge γ_j. The local basis functions $\psi_{j,T}$, $j = 1,2,3,4$, fulfill

$$\frac{1}{|\gamma_k|}\int_{\gamma_k} \psi_{j,T} \, \mathrm{d}s = \delta_{jk}, \quad \forall\ j,k = 1,2,3,4. \tag{2.6}$$

Set the local finite element space on an element T as follows:

$$S_h^N(T) = \text{Span}\,\{\psi_{j,T} : j = 1,2,3,4\}. \tag{2.7}$$

It is obvious that on every element $T \in \mathcal{T}_h$, $S_h^N(T) = \Pi_T$.

2.3. Nonconforming IFE Functions. Next, we describe the construction of a local IFE function, denoted by ϕ_T, on a typical interface element $T \in \mathcal{T}_h^I$ whose vertices and edges are given in (2.2) - (2.3).

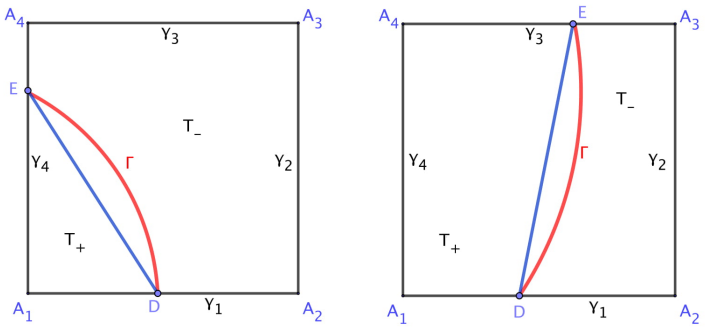

FIG. 2.1. *Type I (left) and Type II (right) interface elements*

Assume that an interface curve Γ intersects $T \in \mathcal{T}_h^I$ at two different points D and E, and the line segment $\overline{DE}$ separates T into two sub-elements T^+ and T^-. Depending on the adjacency of the edges containing D and E, the interface elements will be classified as Type I and Type II interface elements such that these two edges are located at two adjacent edges and at two opposite edges, respectively. See Figure 2.1 for an illustration. We use a Type II interface element to exemplify the construction of the local IFE functions and corresponding spaces, i.e., we assume the interface points are such that

$$D = (x_0 + dh_x, y_0), \quad E = (x_0 + eh_x, y_0 + h_y),$$

where $d, e \in (0,1)$. A local IFE function ϕ_T is defined as a piecewise rotated-Q_1 polynomial as follows:

(2.8)
$$\phi_T(x,y) = \begin{cases} c_1^+ + c_2^+\left(\frac{x-x_0}{h_x}\right) + c_3^+\left(\frac{y-y_0}{h_y}\right) + c_4^+\left(\left(\frac{x-x_0}{h_x}\right)^2 - \left(\frac{y-y_0}{h_y}\right)^2\right) & \text{in } T^+, \\ c_1^- + c_2^-\left(\frac{x-x_0}{h_x}\right) + c_3^-\left(\frac{y-y_0}{h_y}\right) + c_4^-\left(\left(\frac{x-x_0}{h_x}\right)^2 - \left(\frac{y-y_0}{h_y}\right)^2\right) & \text{in } T^-. \end{cases}$$

The coefficients $c_j^{\pm}$ are determined by the mean value v_j on each edge γ_j:

$$\frac{1}{|\gamma_j|}\int_{\gamma_j} \phi_T \, \mathrm{d}s = v_j, \quad j = 1,2,3,4, \tag{2.9}$$

and the following interface jump conditions

$$[\phi_T]_{\overline{DE}} = 0, \tag{2.10}$$

$$\int_{\overline{DE}} [\![\boldsymbol{\nu}_{\overline{DE}} \cdot \beta \nabla \phi_T]\!]_{\overline{DE}} \, \mathrm{d}s = 0, \tag{2.11}$$

where $\boldsymbol{\nu}_{\overline{DE}}$ is the unit normal on $\overline{DE}$. Note that the continuity condition (2.10) is equivalent to

$$[\phi_T(D)] = 0, \quad [\phi_T(E)] = 0, \quad c_4^+ = c_4^-. \tag{2.12}$$

Equations (2.9)–(2.11) provide eight constraints that lead to an 8×8 algebraic system $M_c\mathbf{c} = \mathbf{v}$ on the coefficients $\mathbf{c} = (c_1^-, \cdots, c_4^-, c_1^+, \cdots, c_4^+)^t$ with $\mathbf{v} = (v_1, \cdots, v_4, 0, \cdots, 0)^t$. By direct calculation, one can verify that the matrix M_c is nonsingular for all $\beta^{\pm} > 0$ and $0 < d, e < 1$; see [33] for more details. Hence, an IFE function ϕ_T satisfying jump conditions (2.10) and (2.11) is uniquely determined by its mean values v_j over edges γ_j, $j = 1,2,3,4$. For each $j = 1,2,3,4$, let $\mathbf{v} = \mathbf{v}_j = (v_1, \cdots, v_4, 0, \cdots, 0)^t \in \mathbb{R}^8$ be the j-th canonical vector such that $v_j = 1$ and $v_k = 0$ for $k \neq j$. We can solve for $\mathbf{c}_j = (c_1^-, \cdots, c_4^-, c_1^+, \cdots, c_4^+)^t$ and use it in (2.8) to form the j-th nonconforming rotated-Q_1-IFE local basis function $\phi_{j,T}$. Figure 2.2 provides a comparison of a standard rotated-Q_1-FE basis function and the corresponding rotated-Q_1-IFE basis functions in both Type I and Type II interface elements.

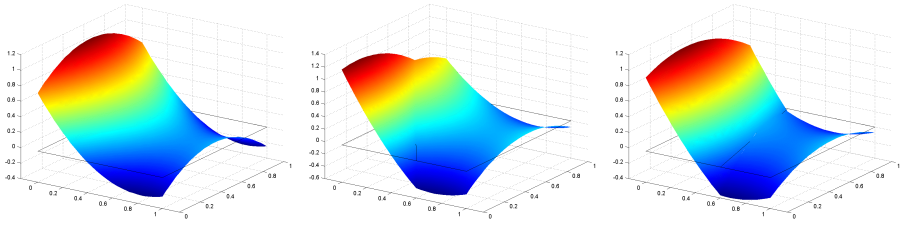

FIG. 2.2. *Nonconforming FE/IFE local basis functions*

Denote by $S_h^I(T) = \text{Span}\{\phi_{j,T} : j = 1,2,3,4\}$ the local rotated-Q_1-IFE space on an interface element T. The global IFE space is defined as follows:

$$S_h(\Omega) = \Big\{ v \in L^2(\Omega) : \ v|_T \in S_h^N(T) \text{ if } T \in \mathcal{T}_h^N, v|_T \in S_h^I(T) \text{ if } T \in \mathcal{T}_h^I; \\ \int_\gamma [v]_\gamma ds = 0 \text{ for all interior edges } \gamma \text{ of } \mathcal{T}_h \Big\}. \tag{2.13}$$

2.4. Basic Properties of IFE Spaces. In this subsection, we summarize some basic properties for the IFE space $S_h(\Omega)$. The results can be verified via straightforward calculations. We also refer readers to Section 3.1 in [33] for proofs of the following lemmas and theorems.

LEMMA 2.1. **(Unisolvency)** *On each interface element $T \in \mathcal{T}_h^I$, an IFE function $\phi_T \in S_h^I(T)$ is uniquely determined by its mean values* (2.9) *and jump conditions* (2.10)-(2.11).

LEMMA 2.2. **(Continuity)** *On each interface element $T \in \mathcal{T}_h^I$, the local IFE space $S_h^I(T) \subset C^0(T)$.*

LEMMA 2.3. **(Partition of Unity)** *On each interface element $T \in \mathcal{T}_h^I$, the IFE basis functions $\phi_{j,T}$ satisfy the partition-of-unity property,* i.e.*,*

$$\sum_{j=1}^{4} \phi_{j,T}(x,y) = 1, \quad \forall (x,y) \in T. \tag{2.14}$$

LEMMA 2.4. **(Consistency)** *On each interface element $T \in \mathcal{T}_h^I$, the IFE basis functions are consistent to standard FE basis functions in the following sense:*

1. *If there is no jump in the coefficient, i.e., $\beta^+ = \beta^-$, then the IFE basis functions $\phi_{j,T}$ become the standard FE basis functions $\psi_{j,T}$.*
2. *If $\min\{|T^+|, |T^-|\}$ shrinks to zero, then the IFE basis functions $\phi_{j,T}$ become the standard FE basis functions $\psi_{j,T}$. Here, $|T^s|$ denotes the area of T^s, $s = +, -$.*

LEMMA 2.5. **(Flux continuity on Γ)** *On each interface element $T \in \mathcal{T}_h^I$, every IFE function $\phi_T \in S_h^I(T)$ satisfies the flux jump condition weakly as follows:*

$$\int_{\Gamma \cap T} [\![\boldsymbol{\nu} \cdot \beta \nabla \phi_T]\!]_{\Gamma \cap T} ds = 0,$$

where $\boldsymbol{\nu}$ is the unit normal to Γ.

LEMMA 2.6. **(Boundedness)** *There exists a constant C, independent of interface location, such that for $j = 1, 2, 3, 4$, and $k = 0, 1, 2$,*

$$\|\phi_{j,T}\|_{\tilde{W}^{k,\infty}(T)} \leq C h_T^{-k} \quad \forall T \in \mathcal{T}_h^I. \tag{2.15}$$

THEOREM 2.7. **(Trace Inequality)** *There exists a constant $C > 0$ independent of interface location, but may depend on the diffusion coefficient β, such that*

$$\|\boldsymbol{\nu} \cdot \beta \nabla v\|_{L^2(\gamma)} \leq C h_T^{-\frac{1}{2}} \|\nabla v\|_{L^2(T)} \quad \forall v \in S_h^I(T) \tag{2.16}$$

where γ is any edge of T, and $\boldsymbol{\nu}$ is the unit outward normal to T.

THEOREM 2.8. **(Inverse Inequality)** *There exists a constant C, independent of interface location, but may depend on the diffusion coefficient β, such that for $0 \leq l \leq k \leq 2$*

$$|v|_{\tilde{W}^{k,\infty}(T)} \leq C h_T^{-1} |v|_{\tilde{H}^k(T)}, \quad |v|_{\tilde{H}^k(T)} \leq C h_T^{l-k} |v|_{\tilde{H}^l(T)}, \quad \forall v \in S_h^I(T). \tag{2.17}$$

3. The Interpolation Operator and Approximation Capability. In this section, we discuss the approximation capability for the nonconforming IFE space $S_h(\Omega)$. On each non-interface element $T \in \mathcal{T}_h^N$, the local interpolation is defined canonically by $\mathcal{I}_T : C(\overline{T}) \to S_h^N(T)$, such that,

$$\mathcal{I}_T u = \sum_{i=1}^{4} \left(\frac{1}{|\gamma_i|} \int_{\gamma_i} u \ \mathrm{ds} \right) \psi_{i,T}, \tag{3.1}$$

where γ_j, $j = 1, 2, 3, 4$ denote the edges of T. The standard scaling argument leads to the following error estimates [31, Lemma 1]:

$$\|\mathcal{I}_T u - u\|_{L^2(T)} + h|\mathcal{I}_T u - u|_{H^1(T)} \leq Ch^2 |u|_{H^2(T)}. \tag{3.2}$$

On each interface element $T \in \mathcal{T}_h^I$, the interpolation operator $\mathcal{I}_T : C(\overline{T}) \to S_h^I(T)$ is defined similarly as follows:

$$\mathcal{I}_T u = \sum_{i=1}^{4} \left(\frac{1}{|\gamma_i|} \int_{\gamma_i} u \ \mathrm{ds} \right) \phi_{i,T}. \tag{3.3}$$

Finally, we define the global IFE interpolation $\mathcal{I}_h : C(\overline{\Omega}) \to S_h(\Omega)$ piecewisely such that

$$(\mathcal{I}_h u)|_T = \mathcal{I}_T u \quad \forall\ T \in \mathcal{T}_h.$$

The error estimates for the interpolation operator on interface elements are reported in [11, 12, 33]. We only state the results in the following theorems.

THEOREM 3.1. *There exists a constant $C > 0$, independent of interface location, such that*

$$\|\mathcal{I}_T u - u\|_{L^2(T)} + h|\mathcal{I}_T u - u|_{H^1(T)} \leq Ch^2 \|u\|_{\widetilde{H}^2(T)} \quad \forall u \in \widetilde{H}^2_\beta(T), \tag{3.4}$$

on every interface element $T \in \mathcal{T}_h^I$.

THEOREM 3.2. *There exists a constant $C > 0$ such that the following interpolation error estimate holds:*

$$\|\mathcal{I}_h u - u\|_{L^2(\Omega)} + h \left(\sum_{T \in \mathcal{T}_h} |\mathcal{I}_T u - u|^2_{H^1(T)} \right)^{\frac{1}{2}} \leq Ch^2 \|u\|_{\widetilde{H}^2(\Omega)} \quad \forall u \in \widetilde{H}^2_\beta(\Omega). \tag{3.5}$$

4. The IFE Galerkin Method and Error Estimates. In this section, we consider a nonconforming IFE Galerkin method and carry out its error estimation.

4.1. The nonconforming IFE Galerkin method. Given a mesh $\mathcal{T}_h$, we denote by $\mathcal{E}_h$, $\mathring{\mathcal{E}}_h$ and $\mathcal{E}_h^b$ the set of all edges, interior edges, and boundary edges, respectively. The sets of interface edges and non-interface edges are denoted by $\mathcal{E}_h^I$ and $\mathcal{E}_h^N$, respectively. For the sake of simplicity, in the following discussion, we assume that the interface curve Γ does not intersect the boundary $\partial\Omega$. Consequently, $\mathcal{E}_h^b \subset \mathcal{E}_h^N$.

Define the bilinear and linear forms

$$a_h(u, v) = \sum_{T \in \mathcal{T}_h} \int_T \beta \nabla u \cdot \nabla v \ \mathrm{dx}, \quad L(v) = \sum_{T \in \mathcal{T}_h} \int_T f v \ \mathrm{dx}.$$

Define the trial function set and test function spaces as follows

$$S_{h,g}(\Omega) = \{v \in S_h(\Omega) : \int_\gamma v \ \mathrm{ds} = \int_\gamma g \ \mathrm{ds}, \ \forall \gamma \in \mathcal{E}_h^b\},$$
$$\mathring{S}_h(\Omega) = \{v \in S_h(\Omega) : \int_\gamma v \ \mathrm{ds} = 0, \ \forall \gamma \in \mathcal{E}_h^b\}.$$

The nonconforming IFE Galerkin method is: find $u_h \in S_{h,g}(\Omega)$ such that

$$a_h(u_h, v_h) = L(v_h), \quad \forall \ v_h \in \mathring{S}_h(\Omega). \tag{4.1}$$

In the following, we derive the error estimation of IFE approximation (4.1).

4.2. Projection operators. For convenience in the analysis to follow, let

$$\gamma_{jk} = \partial T_j \cap \partial T_k, \quad \gamma_j = \partial T_j \cap \partial\Omega, \quad \forall\, T_j, T_k \in \mathcal{T}_h,$$

and write

$$v_j = v|_{T_j} \quad \forall\, T_j \in \mathcal{T}_h; \quad v_{jk} = v_j|_{\gamma_{jk}} \quad \forall \gamma_{jk} \in \mathcal{E}_h^I.$$

Set

$$\Lambda^h = \Big\{\lambda \mid \lambda = (\lambda_{jk}, \lambda_{kj}) \in (\mathcal{P}_0(\gamma_{jk}))^2, \lambda_{jk} + \lambda_{kj} = 0 \ \ \forall \gamma_{jk} \in \mathring{\mathcal{E}}_h; \\ \lambda = \lambda_j \in \mathcal{P}_0(\gamma_j) \ \ \forall \gamma_j \in \mathcal{E}_h^b\Big\}.$$

Denote by $\boldsymbol{\nu}_j$ the unit outward normal to T_j. We will use the following projection operators introduced in [8]: $\Pi_0 : \prod\limits_{\gamma\in\mathcal{E}_h} L^2(\gamma) \to \prod\limits_{\gamma\in\mathcal{E}_h} \mathcal{P}_0(\gamma)$ and $\Pi_{\boldsymbol{\nu}} : \widetilde{H}^2_\beta(\Omega) \to \Lambda^h$ by

$$\langle v - \Pi_0 v, 1\rangle_\gamma = 0 \quad \forall v \in L^2(\gamma) \quad \forall \gamma \in \mathcal{E}_h, \tag{4.2}$$

$$\left\langle \beta \frac{\partial v_j}{\partial \boldsymbol{\nu}_j} - \Pi_{\boldsymbol{\nu}} v, 1 \right\rangle_{\gamma_{jk}} = 0 \quad \forall v \in \widetilde{H}^2_\beta(\Omega) \quad \forall \gamma_{jk} \in \mathcal{E}_h, \tag{4.3}$$

so that $\Pi_0^\gamma(v) := \Pi_0(v|_\gamma) = \frac{1}{|\gamma|}\int_\gamma v \ \mathrm{ds}$ is the average of v over γ and

$$\left(\Pi_{\boldsymbol{\nu}} v|_{\gamma_{jk}}, \Pi_{\boldsymbol{\nu}} v|_{\gamma_{kj}}\right) = \left(\Pi_0^{\gamma_{jk}} \beta \frac{\partial v_j}{\partial \boldsymbol{\nu}_j}, \Pi_0^{\gamma_{kj}} \beta \frac{\partial v_k}{\partial \boldsymbol{\nu}_k}\right) \in \mathbb{R}^2 \quad \forall \gamma_{jk} \in \mathcal{E}_h^I.$$

Lemma 4.1. *Let $\gamma = (0, h)$ with $\gamma^- = (0, \alpha)$ and $\gamma^+ = (\alpha, h)$. Assume that $u \in L^2(\gamma)$ and $u|_{\gamma^s} \in H^{\frac{1}{2}}(\gamma^s), s = -, +$. Then $u \in H^{\frac{1}{2}-\epsilon}(\gamma)$ for every $\epsilon \in (0, \frac{1}{4})$. Moreover, there exists a constant C independent of α, such that*

$$\|u\|_{H^{\frac{1}{2}-\epsilon}(\gamma)} \le \frac{C}{\sqrt{\epsilon}} \left(\|u\|_{H^{\frac{1}{2}}(\gamma^-)} + \|u\|_{H^{\frac{1}{2}}(\gamma^+)}\right).$$

Proof. For every $\epsilon \in (0, \frac{1}{4})$, let $\sigma = \frac{1}{2} - \epsilon$, then $\sigma \in (\frac{1}{4}, \frac{1}{2})$. For $q \ge 1$ and $y \in \gamma^-$,

$$\int_{\gamma^+} \frac{1}{|x-y|^{(1+2\sigma)q}} dx = \frac{(h-y)^{1-(1+2\sigma)q} - (\alpha - y)^{1-(1+2\sigma)q}}{1-(1+2\sigma)q}.$$

Since $\sigma \in (\frac{1}{4}, \frac{1}{2})$, we specifically choose

$$q = \frac{1}{2}\left(1 + \frac{2}{1+2\sigma}\right) \quad \Longrightarrow \quad q = \frac{2-\epsilon}{2(1-\epsilon)}.$$

Then $1 \le q < \frac{2}{1+2\sigma}$, $1-(1+2\sigma)q \neq -1$, and $1+2\sigma \le (1+2\sigma)q < 2$. Hence,

$$\begin{aligned}
&I(\gamma^-, \gamma^+, \sigma, q) := \int_{\gamma^-}\int_{\gamma^+} \frac{1}{|x-y|^{(1+2\sigma)q}} dxdy \\
&= \left(\frac{1}{1-(1+2\sigma)q}\right)\left(\frac{1}{2-(1+2\sigma)q}\right)\left(h^{2-(1+2\sigma)q} - (h-\alpha)^{2-(1+2\sigma)q} - \alpha^{2-(1+2\sigma)q}\right) \\
&\le C\left|\frac{1}{1-(1+2\sigma)q}\right|\left|\frac{1}{2-(1+2\sigma)q}\right| = C\left|\frac{1}{1-\epsilon}\right|\left|\frac{1}{\epsilon}\right| \le \frac{C}{\epsilon}.
\end{aligned}$$

Therefore, using p such that $\frac{1}{p} + \frac{1}{q} = 1$, and the above estimate, we have

$$\begin{aligned}
&\int_{\gamma^-}\int_{\gamma^+} \frac{|u(x)-u(y)|^2}{|x-y|^{1+2\sigma}} dxdy \\
&\le \int_{\gamma^-}\left(\left[\int_{\gamma^+} |u(x)-u(y)|^{2p} dx\right]^{\frac{1}{2p}}\right)^2 \left[\int_{\gamma^+} \frac{1}{|x-y|^{(1+2\sigma)q}} dx\right]^{\frac{1}{q}} dy \\
&\le 2\int_{\gamma^-} \|u\|^2_{L^{2p}(\gamma^+)} \left[\int_{\gamma^+} \frac{1}{|x-y|^{(1+2\sigma)q}} dx\right]^{\frac{1}{q}} dy + 2\int_{\gamma^-} |u(y)|^2 \left[\int_{\gamma^+} \frac{1}{|x-y|^{(1+2\sigma)q}}\ \mathrm{dx}\right]^{\frac{1}{q}} dy. \\
&\le 2\|u\|^2_{L^{2p}(\gamma^+)} \left(\int_{\gamma^-} 1^p dy\right)^{\frac{1}{p}} I(\gamma^-, \gamma^+, \sigma, q)^{\frac{1}{q}} + 2\left(\int_{\gamma^-} |u(y)|^{2p} dy\right)^{\frac{1}{p}} I(\gamma^-, \gamma^+, \sigma, q)^{\frac{1}{q}} \\
&\le C\|u\|^2_{L^{2p}(\gamma^+)} \left(\frac{1}{\epsilon}\right)^{\frac{1}{q}} + C\|u\|^2_{L^{2p}(\gamma^-)} \left(\frac{1}{\epsilon}\right)^{\frac{1}{q}} \\
&\le C\left(\frac{1}{\epsilon}\right)^{\frac{2(1-\epsilon)}{2-\epsilon}} \left(\|u\|^2_{H^{\frac{1}{2}}(\gamma^+)} + \|u\|^2_{H^{\frac{1}{2}}(\gamma^-)}\right).
\end{aligned}$$

In the last step, we used the Sobolev embedding theorem for one dimension:

$$W^{\frac{1}{2},2}(\gamma^s) \hookrightarrow W^{0,p}(\overline{\gamma^s}), \quad s = -, +, \quad p \in [1, \infty).$$

By definition of the fractional Sobolev norm, we have

$$\begin{aligned}
&\|u\|^2_{H^\sigma(\gamma)} = \|u\|^2_{L^2(\gamma)} + \int_\gamma\int_\gamma \frac{|u(x)-u(y)|^2}{|x-y|^{1+2\sigma}} dxdy \\
&= \|u\|^2_{L^2(\gamma)} + \int_{\gamma^-}\int_{\gamma^-} \frac{|u(x)-u(y)|^2}{|x-y|^{1+2\sigma}} dxdy + 2\int_{\gamma^-}\int_{\gamma^+} \frac{|u(x)-u(y)|^2}{|x-y|^{1+2\sigma}} dxdy \\
&\qquad + \int_{\gamma^+}\int_{\gamma^+} \frac{|u(x)-u(y)|^2}{|x-y|^{1+2\sigma}} dxdy \\
&\le \|u\|^2_{H^{\frac{1}{2}}(\gamma^+)} + \|u\|^2_{H^{\frac{1}{2}}(\gamma^-)} + C\left(\frac{1}{\epsilon}\right)^{\frac{2(1-\epsilon)}{2-\epsilon}} \left(\|u\|^2_{H^{\frac{1}{2}}(\gamma^+)} + \|u\|^2_{H^{\frac{1}{2}}(\gamma^-)}\right),
\end{aligned}$$

which leads to

$$\|u\|_{H^\sigma(\gamma)} \le \frac{C}{\epsilon^{(1-\epsilon)/(2-\epsilon)}} \left(\|u\|_{H^{\frac{1}{2}}(\gamma^-)} + \|u\|_{H^{\frac{1}{2}}(\gamma^+)}\right) \le \frac{C}{\sqrt{\epsilon}} \left(\|u\|_{H^{\frac{1}{2}}(\gamma^-)} + \|u\|_{H^{\frac{1}{2}}(\gamma^+)}\right),$$

because for small ϵ, we have

$$\frac{1-\epsilon}{2-\epsilon} = \frac{1}{2} - \frac{\epsilon}{4} - \frac{\epsilon^2}{8} - \frac{\epsilon^3}{16} - \cdots \leq \frac{1}{2}.$$

□

THEOREM 4.2. *Let $T \in \mathcal{T}_h$ and γ be an edge of T. Then there exists a constant $C > 0$ such that the following hold on a mesh $\mathcal{T}_h$ with a sufficiently small mesh size:*

1. *If $T \in \mathcal{T}_h^N$ and $v \in H^2(T) + S_h^N(T)$, then*

$$\left\| \beta \frac{\partial v}{\partial \boldsymbol{\nu}} - \Pi_{\boldsymbol{\nu}} v \right\|_{L^2(\gamma)} \leq C h^{\frac{1}{2}} \|v\|_{H^2(T)}.$$

2. *If $\gamma \in \mathcal{E}_h^N$ but $T \in \mathcal{T}_h^I$, and $v \in \widetilde{H}_\beta^2(T) + S_h^I(T)$, then*

$$\left\| \beta \frac{\partial v}{\partial \boldsymbol{\nu}} - \Pi_{\boldsymbol{\nu}} v \right\|_{L^2(\gamma)} \leq C h^{\frac{1}{2}} \left(\|v\|_{H^2(\widetilde{T}^-)} + \|v\|_{H^2(\widetilde{T}^+)} \right).$$

3. *If $\gamma \in \mathcal{E}_h^I$ and $v \in \widetilde{H}_\beta^2(T) + S_h^I(T)$, then*

$$\left\| \beta \frac{\partial v}{\partial \boldsymbol{\nu}} - \Pi_{\boldsymbol{\nu}} v \right\|_{L^2(\gamma)} \leq C h^{\frac{1}{2}} |\log h|^{\frac{1}{2}} \left(\|v\|_{H^2(\widetilde{T}^-)} + \|v\|_{H^2(\widetilde{T}^+)} \right).$$

Here, for $T \in \mathcal{T}_h^I$, designate

$$\widetilde{T}^s = \begin{cases} T \cap \Omega^s & \text{for } v \in \widetilde{H}_\beta^2(T), \\ T^s & \text{for } v \in S_h^I(T), \end{cases} \qquad \text{for } s = +, -.$$

Proof. Let $\gamma \in \mathcal{E}_h$. In the first two cases we assume $\gamma \in \mathcal{E}_h^N$, but for the third case we assume $\gamma \in \mathcal{E}_h^I$. Then by the standard trace theorem or the lemma above, we have $\beta \frac{\partial v}{\partial \boldsymbol{\nu}} \in H^{\frac{1}{2}}(\gamma)$ or $\beta \frac{\partial v}{\partial \boldsymbol{\nu}} \in H^{\frac{1}{2}-\epsilon}(\gamma)$ for any $\epsilon \in (0, \frac{1}{4})$.

Since $\Pi_{\boldsymbol{\nu}} v$ is the L^2 projection of $\beta \frac{\partial v}{\partial \boldsymbol{\nu}}$ to the space of constant polynomials, applying the error estimate for polynomial projection and the standard error estimate on interpolation of Sobolev spaces (see [9, Theorem 1.4, p.6]), we have

$$\left\| \beta \frac{\partial v}{\partial \boldsymbol{\nu}} - \Pi_{\boldsymbol{\nu}} v \right\|_{L^2(\gamma)} \leq \begin{cases} C h^{\frac{1}{2}} \left\| \beta \frac{\partial v}{\partial \boldsymbol{\nu}} \right\|_{H^{\frac{1}{2}}(\gamma)} & \text{if } \gamma \in \mathcal{E}_h^N, \\ C h^{\frac{1}{2}-\epsilon} \left\| \beta \frac{\partial v}{\partial \boldsymbol{\nu}} \right\|_{H^{\frac{1}{2}-\epsilon}(\gamma)} & \text{if } \gamma \in \mathcal{E}_h^I. \end{cases} \tag{4.4}$$

For the first two cases, by the definition of the $H^{1/2}$-norm for the zero-th order trace of a H^1 function, see for example [2], we have

$$\left\| \beta \frac{\partial v}{\partial \boldsymbol{\nu}} \right\|_{H^{\frac{1}{2}}(\gamma)} \leq \begin{cases} \left\| \beta \frac{\partial v}{\partial \boldsymbol{\nu}} \right\|_{H^1(T)} & \text{if } T \in \mathcal{T}_h^N, \\ \left\| \beta \frac{\partial v}{\partial \boldsymbol{\nu}} \right\|_{H^1(\widetilde{T}^s)} \leq \left\| \beta \frac{\partial v}{\partial \boldsymbol{\nu}} \right\|_{H^1(\widetilde{T}^-)} + \left\| \beta \frac{\partial v}{\partial \boldsymbol{\nu}} \right\|_{H^1(\widetilde{T}^+)} & \text{if } T \in \mathcal{T}_h^I, \end{cases}$$

which means

$$\left\| \beta \frac{\partial v}{\partial \boldsymbol{\nu}} \right\|_{H^{\frac{1}{2}}(\gamma)} \leq \begin{cases} \max\{\beta^+, \beta^-\} \|v\|_{H^2(T)} & \text{if } T \in \mathcal{T}_h^N, \\ \max\{\beta^+, \beta^-\} \|v\|_{\widetilde{H}^2(T)} & \text{if } T \in \mathcal{T}_h^I. \end{cases} \tag{4.5}$$

For the third case, applying Lemma 4.1, we have

$$\begin{aligned}\left\|\beta\frac{\partial v}{\partial \boldsymbol{\nu}}\right\|_{H^{\frac{1}{2}-\epsilon}(\gamma)} &\le \frac{C}{\sqrt{\epsilon}}\left(\|\beta\frac{\partial v}{\partial \boldsymbol{\nu}}\|_{H^{\frac{1}{2}}(\gamma^-)}+\|\beta\frac{\partial v}{\partial \boldsymbol{\nu}}\|_{H^{\frac{1}{2}}(\gamma^+)}\right)\\ &\le \frac{C}{\sqrt{\epsilon}}\left(\|v\|_{H^2(\widetilde{T}^-)}+\|v\|_{H^2(\widetilde{T}^+)}\right). \qquad (4.6)\end{aligned}$$

Finally, all the estimates in this theorem follow by applying (4.5) and (4.6) to (4.4), and by taking the minimum of $\frac{1}{h^\epsilon\sqrt{\epsilon}}$ over $0<\epsilon<1/4$. Indeed, at $\epsilon=\frac{1}{2\log\frac{1}{h}}$, for $0<h<\frac{1}{e^2}$, the minimum value is

$$\frac{1}{h^\epsilon\sqrt{\epsilon}} = h^{\frac{1}{2\log h}}\sqrt{2\log\frac{1}{h}} = \sqrt{2e}|\log h|^{\frac{1}{2}}.$$

□

4.3. The Energy-Norm Error Estimate. Define the (broken) energy norm

$$|\!|\!| u |\!|\!| = \sqrt{a_h(u,u)}.$$

As needed, we quote the following second Strang lemma for the IFE solution:

LEMMA 4.3. *Let $u\in\widetilde{H}^1_\Gamma(\Omega)$ and $u_h\in S_h(\Omega)$ be the solutions of* (2.1) *and* (4.1)*, respectively. Then,*

$$|\!|\!| u-u_h |\!|\!| \le C\left\{\inf_{v_h\in S_h(\Omega)}|\!|\!| u-v_h |\!|\!| + \sup_{w_h\in S_h(\Omega)}\frac{|a_h(u,w_h)-L(w_h)|}{|\!|\!| w_h |\!|\!|}\right\}. \qquad (4.7)$$

We are now ready to state and derive an error estimate in the energy norm.

THEOREM 4.4. *Let $u\in\widetilde{H}^2_\beta(\Omega)$ and $u_h\in S_h(\Omega)$ be the solutions of* (2.1) *and* (4.1)*, respectively. Then, there exists a constant C such that*

$$|\!|\!| u-u_h |\!|\!| \le Ch\left(\|u\|_{\widetilde{H}^2(\Omega)}+|\log h|^{\frac{1}{2}}\sum_{T\in\mathcal{T}_h^I}\|u\|_{\widetilde{H}^2(T)}\right). \qquad (4.8)$$

If, in addition, $u\in\widetilde{W}^{2,q}_\beta(\Omega)$ for some $q>2$, then there exists $h_0>0$ such that, for all $0<h<h_0$,

$$|\!|\!| u-u_h |\!|\!| \le Ch\Big(\|u\|_{\widetilde{H}^2(\Omega)}+\sum_{T\in\mathcal{T}_h^I}\|u\|_{\widetilde{W}^{2,q}(T)}\Big). \qquad (4.9)$$

Proof. We need to estimate those terms bounding $|\!|\!| u-u_h |\!|\!|$ in (4.7) of the Strang lemma above. By the interpolation estimate (3.5), we can estimate the first term on the right hand side of (4.7) as follows:

$$\inf_{v_h\in S_h(\Omega)}|\!|\!| u-v_h |\!|\!| \le Ch\|u\|_{\widetilde{H}^2(\Omega)}. \qquad (4.10)$$

Next, let $w_h\in S_h(\Omega)$ be arbitrary. Then, since $u\in H^1(\Omega)$, it follows that

$$\begin{aligned}a_h(u,w_h) &= \sum_j(\beta\nabla u,\nabla w_h)_{T_j} = -\sum_j(\nabla\cdot\beta\nabla u,w_h)_{T_j}+\sum_j\left\langle\beta\frac{\partial u_j}{\partial\boldsymbol{\nu}_j},w_h\right\rangle_{\partial T_j}\\ &= (-\nabla\cdot\beta\nabla u,w_h)+\sum_j\left\langle\beta\frac{\partial u_j}{\partial\boldsymbol{\nu}_j},w_h\right\rangle_{\partial T_j}.\end{aligned}$$

Hence, by choosing $m_j \in \mathcal{P}_0(T_j)$ to be the the average of w_h over T_j, one sees that

$$\begin{aligned} a_h(u,w_h) - L(w_h) &= \sum_j \left\langle \beta \frac{\partial u_j}{\partial \boldsymbol{\nu}_j}, w_h \right\rangle_{\partial T_j} = \sum_j \left\langle \beta \frac{\partial u_j}{\partial \boldsymbol{\nu}_j} - \Pi_{\boldsymbol{\nu}} u_j, w_h \right\rangle_{\partial T_j} \\ &= \sum_j \left\langle \beta \frac{\partial u_j}{\partial \boldsymbol{\nu}_j} - \Pi_{\boldsymbol{\nu}} u_j, w_h - m_j \right\rangle_{\partial T_j}. \end{aligned} \tag{4.11}$$

Hence, by Theorem 4.2, the trace inequality on T_j, and the approximation capability of m_j, we have

$$\begin{aligned} &|a_h(u,w_h) - L(w_h)| \\ &\le \Big(\sum_j \Big\| \beta \frac{\partial u_j}{\partial \boldsymbol{\nu}_j} - \Pi_{\boldsymbol{\nu}} u_j \Big\|^2_{L^2(\partial T_j)} \Big)^{\frac{1}{2}} \Big(\sum_j \|w_h - m_j\|^2_{L^2(\partial T_j)} \Big)^{\frac{1}{2}} \\ &\le Ch^{\frac{1}{2}} \Big(\sum_{T\in\mathcal{T}_h^N} \|u\|_{H^2(T)} + |\log h|^{\frac{1}{2}} \sum_{T\in\mathcal{T}_h^I} \|u\|_{\widetilde{H}^2(T)} \Big) Ch^{\frac{1}{2}} \Big(\sum_j \|\nabla w_h\|^2_{L^2(T_j)} \Big)^{\frac{1}{2}} \\ &\le Ch \Big(\sum_{T\in\mathcal{T}_h^N} \|u\|_{H^2(T)} + |\log h|^{\frac{1}{2}} \sum_{T\in\mathcal{T}_h^I} \|u\|_{\widetilde{H}^2(T)} \Big) |\!|\!| w_h |\!|\!|. \end{aligned} \tag{4.12}$$

Then, applying (4.10) and (4.12) to (4.7) leads to (4.8).

Assume that $u \in \widetilde{W}^{2,q}_\beta(\Omega)$ for some $q > 2$. Then choose p such that $\frac{1}{p} + \frac{2}{q} = 1$, so that, for $T \in \mathcal{T}_h^I$

$$\begin{aligned} \|u\|_{\widetilde{H}^2(T)} &\le \Big(\sum_{s=\pm} \int_{T^s} \sum_{|\alpha|\le 2} |D^\alpha u|^2 dx \Big)^{\frac{1}{2}} \le \Big(\int_T 1^p dx \Big)^{\frac{1}{2p}} \Big(\sum_{s=\pm} \int_{T^s} \Big(\sum_{|\alpha|\le 2} |D^\alpha u|^2 \Big)^{\frac{q}{2}} dx \Big)^{\frac{1}{q}} \\ &\le C|T|^{\frac{1}{2p}} \Big(\sum_{s=\pm} \int_{T^s} \sum_{|\alpha|\le 2} |D^\alpha u|^q dx \Big)^{\frac{1}{q}} \le Ch^{\frac{1}{p}} \|u\|_{\widetilde{W}^{2,q}(T)}. \end{aligned}$$

Hence, the second term in (4.8) can be bounded by

$$|\log h|^{\frac{1}{2}} \sum_{T\in\mathcal{T}_h^I} \|u\|_{\widetilde{H}^2(T)} \le C \sum_{T\in\mathcal{T}_h^I} |\log h|^{\frac{1}{2}} h^{\frac{1}{p}} \|u\|_{\widetilde{W}^{2,q}(T)}.$$

Since $\lim_{h\to 0} |\log h|^{\frac{1}{2}} h^{\frac{1}{p}} = 0$, there exists $h_0 > 0$ such that the estimate (4.9) is valid for $0 < h < h_0$. This completes the proof. ∎

REMARK 4.1. *Indeed,* (4.8) *implies that the IFE solution converge faster than* $\mathcal{O}(h|\log h|^{\frac{1}{2}})$*, since its multiplication factor,* $\sum_{T\in\mathcal{T}_h^I} \|u\|_{\widetilde{H}^2(T)}$*, goes to zero as* $h \to 0$*.*

4.4. Duality and the L^2-Error Estimate. Let

$$\eta_h = \mathcal{I}_h u - u_h \in \mathring{S}_h(\Omega),$$

and let $\psi \in \widetilde{H}^2_\beta(\Omega)$ be the solution of the dual problem:

$$-\nabla\cdot(\beta\nabla\psi) = \eta_h \quad \text{in } \Omega, \tag{4.13a}$$

$$\psi = 0 \quad \text{on } \partial\Omega. \tag{4.13b}$$

Assume that the interface problem (2.1) is $\widetilde{H}^2_\beta(\Omega)$-regular so that the elliptic regularity estimate holds:

$$\|\psi\|_{\widetilde{H}^2(\Omega)} \le C\|\eta_h\|_{L^2(\Omega)}. \tag{4.14}$$

We start from recalling the following standard estimates for the IFE interpolation $\mathcal{I}_h\psi$: there exists a constant C such that

$$\begin{cases} \|\mathcal{I}_h\psi\|_{H^2(T)} \le C\,\|\psi\|_{H^2(T)} & \forall\ T \in \mathcal{T}_h^N, \\ \|\mathcal{I}_h\psi\|_{H^2(T_j^-)} + \|\mathcal{I}_h\psi\|_{H^2(T_j^+)} \le C\,\|\psi\|_{\widetilde{H}^2(T)} & \forall\ T \in \mathcal{T}_h^I. \end{cases} \tag{4.15}$$

Since $\eta_h \in \mathring{S}_h(\Omega)$, it follows that

$$\begin{aligned} \|\eta_h\|^2_{L^2(\Omega)} &= (-\nabla\cdot\beta\nabla\psi, \eta_h) = a_h(\psi,\eta_h) - \sum_j \left\langle \beta\frac{\partial\psi_j}{\partial\boldsymbol{\nu}_j}, \eta_{h_j}\right\rangle_{\partial T_j} \\ &= a_h(\psi,\eta_h) - \sum_j \left\langle \beta\frac{\partial\psi_j}{\partial\boldsymbol{\nu}_j} - \Pi_{\boldsymbol{\nu}}\psi_j, \eta_{h_j} - q_j\right\rangle_{\partial T_j} \quad \text{for all } q_j \in \mathcal{P}_0(T_j). \end{aligned}$$

Next, for all $v_h \in \mathring{S}_h(\Omega)$, similarly to (4.11), we have

$$\begin{aligned} a_h(\eta_h, v_h) &= a_h(u, v_h) - a_h(u_h, v_h) - a_h(u - \mathcal{I}_h u, v_h) \\ &= \sum_j \left\langle \beta\frac{\partial u_j}{\partial\boldsymbol{\nu}_j} - \Pi_{\boldsymbol{\nu}}u_j, v_{h_j}\right\rangle_{\partial T_j} - a_h(u - \mathcal{I}_h u, v_h). \end{aligned}$$

Using the property $[\psi]_{\gamma_{jk}} = 0$ and recalling the definition of $\Pi_{\boldsymbol{\nu}}$, we see that

$$\left\langle \beta\frac{\partial u_j}{\partial\boldsymbol{\nu}_j} - \Pi_{\boldsymbol{\nu}}u_j, \psi_j\right\rangle_{\gamma_{jk}} + \left\langle \beta\frac{\partial u_k}{\partial\boldsymbol{\nu}_k} - \Pi_{\boldsymbol{\nu}}u_k, \psi_k\right\rangle_{\gamma_{kj}} = 0.$$

In addition, note that for $v_h \in S_h(\Omega)$, $-\nabla\cdot(\beta\nabla v_h) = 0$ on every $T \in \mathcal{T}_h$; hence,

$$\begin{aligned} a_h(u - \mathcal{I}_h u, v_h) &= \sum_j (u - \mathcal{I}_h u, -\nabla\cdot(\beta\nabla v_h))_{T_j} + \sum_j \left\langle u - \mathcal{I}_h u, \beta\frac{\partial v_h}{\partial\boldsymbol{\nu}_j}\right\rangle_{\partial T_j} \\ &= \sum_j \left\langle u - \mathcal{I}_h u, \beta\frac{\partial v_h}{\partial\boldsymbol{\nu}_j} - \Pi_{\boldsymbol{\nu}_j} v_h\right\rangle_{\partial T_j}. \end{aligned}$$

Therefore

$$\begin{aligned} \|\eta_h\|^2_{L^2(\Omega)} &= a_h(\psi,\eta_h) - \sum_j \left\langle \beta\frac{\partial\psi_j}{\partial\boldsymbol{\nu}_j} - \Pi_{\boldsymbol{\nu}}\psi_j, \eta_{h_j} - q_j\right\rangle_{\partial T_j} \\ &= a_h(\eta_h, \psi - v_h) - a_h(u - \mathcal{I}_h u, v_h) \\ &\quad - \sum_j \left\langle \beta\frac{\partial\psi_j}{\partial\boldsymbol{\nu}_j} - \Pi_{\boldsymbol{\nu}}\psi_j, \eta_{h_j} - q_j\right\rangle_{\partial T_j} + \sum_j \left\langle \beta\frac{\partial u_j}{\partial\boldsymbol{\nu}_j} - \Pi_{\boldsymbol{\nu}}u_j, v_{h_j} - \psi_j\right\rangle_{\partial T_j} \\ &= a_h(\eta_h, \psi - v_h) - \sum_j \left\langle u - \mathcal{I}_h u, \beta\frac{\partial v_h}{\partial\boldsymbol{\nu}_j} - \Pi_{\boldsymbol{\nu}_j} v_h\right\rangle_{\partial T_j} \\ &\quad - \sum_j \left\langle \beta\frac{\partial\psi_j}{\partial\boldsymbol{\nu}_j} - \Pi_{\boldsymbol{\nu}}\psi_j, \eta_{h_j} - q_j\right\rangle_{\partial T_j} + \sum_j \left\langle \beta\frac{\partial u_j}{\partial\boldsymbol{\nu}_j} - \Pi_{\boldsymbol{\nu}}u_j, v_{h_j} - \psi_j\right\rangle_{\partial T_j}. \end{aligned} \tag{4.16}$$

With these preparations, we are ready to derive the error estimate in the L^2-norm for the IFE solution.

THEOREM 4.5. *Assume that the interface problem* (2.1) *is* $\widetilde{H}^2_\beta(\Omega)$*-regular. Then, there exists a constant* C *such that the* L^2*-norm error of the IFE solution satisfies the following estimate:*

$$\|u-u_h\|_{L^2(\Omega)} \le Ch^2\Big(|\log h|^{\frac{1}{2}}\|u\|_{\widetilde{H}^2(\Omega)} + |\log h|\sum_{T\in\mathcal{T}_h^I}\|u\|_{\widetilde{H}^2(T)}\Big). \tag{4.17}$$

Proof. We proceed to estimate each term on the right hand side of (4.16). First, choose $v_h = \mathcal{I}_h\psi$. Then, by (3.5) and (4.14), the first term on the right-hand side of (4.16) is bounded as follows:

$$|a_h(\eta_h,\psi-v_h)| = |a_h(\eta_h,\psi-\mathcal{I}_h\psi)| \le Ch|\!|\!|\eta_h|\!|\!|\|\eta_h\|_{L^2(\Omega)}. \tag{4.18}$$

Again, choosing $q_j\in\mathcal{P}_0(T_j)$ to be the the average of η_h over T_j, by Theorem 4.2, the trace inequality on T_j, Theorem 3.2, and (4.14), we can bound the last two terms on the right hand side of (4.16) as follows:

$$\begin{aligned}
&\Big|\sum_j\Big\langle\beta\frac{\partial\psi_j}{\partial\boldsymbol{\nu}_j}-\Pi_{\boldsymbol{\nu}}\psi_j,\eta_{h_j}-q_j\Big\rangle_{\partial T_j}\Big| + \Big|\sum_j\Big\langle\beta\frac{\partial u_j}{\partial\boldsymbol{\nu}_j}-\Pi_{\boldsymbol{\nu}}u_j,v_{h_j}-\psi_j\Big\rangle_{\partial T_j}\Big| \\
&\quad\le Ch\Big(\sum_{T\in\mathcal{T}_h^N}\|\psi\|_{H^2(T)}+|\log h|^{\frac{1}{2}}\sum_{T\in\mathcal{T}_h^I}\|\psi\|_{\widetilde{H}^2(T)}\Big)|\!|\!|\eta_h|\!|\!| \\
&\qquad +Ch^2\Big(\sum_{T\in\mathcal{T}_h^N}\|u\|_{H^2(T)}+|\log h|^{\frac{1}{2}}\sum_{T\in\mathcal{T}_h^I}\|u\|_{\widetilde{H}^2(T)}\Big)\|\psi\|_{\widetilde{H}^2(\Omega)} \\
&\quad\le Ch\Big(|\log h|^{\frac{1}{2}}|\!|\!|\eta_h|\!|\!| + h\sum_{T\in\mathcal{T}_h^N}\|u\|_{H^2(T)}+h|\log h|^{\frac{1}{2}}\sum_{T\in\mathcal{T}_h^I}\|u\|_{\widetilde{H}^2(T)}\Big)\|\eta_h\|_{L^2(\Omega)}.
\end{aligned} \tag{4.19}$$

For the second term in (4.16), by Theorem 3.2, Theorem 4.2, (4.15) and (4.14),

$$\begin{aligned}
&\Big|\sum_j\Big\langle u-\mathcal{I}_hu,\beta\frac{\partial v_{h_j}}{\partial\boldsymbol{\nu}_j}-\Pi_{\boldsymbol{\nu}_j}v_h\Big\rangle_{\partial T_j}\Big| \\
&\le\Big(\sum_j|u-\mathcal{I}_hu|^2_{0,\partial T_j}\Big)^{\frac{1}{2}}\Big(\sum_j\Big|\beta\frac{\partial v_{h_j}}{\partial\boldsymbol{\nu}_j}-\Pi_{\boldsymbol{\nu}_j}v_h\Big|^2_{0,\partial T_j}\Big)^{\frac{1}{2}} \\
&\le Ch^{\frac{3}{2}}\|u\|_{\widetilde{H}^2(\Omega)}\Big(h\sum_{T\in\mathcal{T}_h^N}\|v_h\|^2_{H^2(T)}+h|\log h|\sum_{T\in\mathcal{T}_h^I}\|v_h\|^2_{\widetilde{H}^2(T)}\Big)^{\frac{1}{2}} \\
&\le Ch^2|\log h|^{\frac{1}{2}}\|u\|_{\widetilde{H}^2(\Omega)}\|\eta_h\|_{L^2(\Omega)}.
\end{aligned} \tag{4.20}$$

Plugging the estimates (4.18)–(4.20) in (4.16) gives

$$\begin{aligned}
\|\eta_h\|_{L^2(\Omega)} &\le Ch|\log h|^{\frac{1}{2}}|\!|\!|\eta_h|\!|\!| + Ch^2|\log h|^{\frac{1}{2}}\|u\|_{\widetilde{H}^2(\Omega)} \\
&\le Ch|\log h|^{\frac{1}{2}}\left(|\!|\!|\mathcal{I}_hu-u|\!|\!|+|\!|\!|u-u_h|\!|\!|\right)+Ch^2|\log h|^{\frac{1}{2}}\|u\|_{\widetilde{H}^2(\Omega)}.
\end{aligned}$$

Finally, applying Theorem 3.2 and Theorem 4.4 to the above estimate, we arrive at the desired estimate (4.17). This completes the proof. ∎

REMARK 4.2. *The estimate given in* (4.17) *suggests that the IFE solution converges in* L^2*-norm better than* $\mathcal{O}(h^2|\log h|)$ *which is optimal sans the usual* $|\log h|$

factor.

REMARK 4.3. *An optimal rate $O(h^2)$ without $|\log h|$ factor may be obtained with slightly better regularity $u \in \widetilde{W}_{\beta}^{2,q}(\Omega)$, $q > 2$, and the elliptic regularity assumption based on L^q-norm. In addition, the analysis requires the interpolation error estimates for IFE functions based on L^q-norm, which will be an interesting future work.*

5. Numerical Examples. In this section, we present some numerical examples to demonstrate the performance of the nonconforming Q_1-IFE method for elliptic interface problems. We also compare the numerical results obtained by this IFE method with those obtained by the conforming Q_1-IFE method.

The tests will be performed on different shapes of interfaces. We will use a family of Cartesian meshes $\{\mathcal{T}_h\}_{0<h<1}$, each of which consists of $N \times N$ congruent rectangles. Errors of an IFE approximation are reported in L^∞, L^2, and semi-H^1 norms. Specifically, error in L^∞-norm is calculated using the formula:

$$\|u_h - u\|_{L^\infty} = \max_{T\in\mathcal{T}_h} \left(\max_{(x,y)\in\hat{T}\subset T} |u_h(x,y) - u(x,y)| \right), \tag{5.1}$$

where $\hat{T}$ consists of the 49 uniformly distributed points in T. We also report the condition numbers for the stiffness matrices on each level of mesh.

5.1. Circular Interface. We first test the nonconforming IFE method on the example given in [16, 28]. Let $\Omega = (-1,1)^2$, separated by a circular interface curve Γ centered at the origin with radius $r_0 = \pi/5$ such that

$$\Omega^- = \{(x,y) \in \Omega : x^2 + y^2 < r_0^2\}, \quad \Omega^+ = \{(x,y) \in \Omega : \ x^2 + y^2 > r_0^2\}.$$

The exact solution is chosen as

$$u(x,y) = \begin{cases} \dfrac{r^a}{\beta^-} & \text{if } r < r_0, \\ \dfrac{r^a}{\beta^+} + \left(\dfrac{1}{\beta^-} - \dfrac{1}{\beta^+}\right) r_0^a & \text{if } r > r_0, \end{cases} \tag{5.2}$$

where $a = 5$, $r = \sqrt{x^2 + y^2}$.

Errors of numerical solutions for high coefficient contrasts $(\beta^-, \beta^+) = (1, 1000)$ and $(\beta^-, \beta^+) = (1000, 1)$ are reported in Tables 5.1 and 5.2, respectively. Convergence rates in semi-H^1 norm and L^2-norm confirm our error analysis (4.8) and (4.17). Data in these tables also suggest that the convergence rate in L^∞-norm is approximately second order, which is optimal from the point view of the polynomial degrees of the IFE space. We also note that the condition numbers of the stiffness matrices grow with order $O(h^{-2})$. The numerical solutions for these two coefficient contrasts are plotted in Figure 5.1. Numerical results for small coefficient jumps (e.g. $\beta^- = 1$, $\beta^+ = 10$) are similar, thus we omit those data in the paper.

5.2. Sharp-Corner Interface. In this example, we consider the case when the interface has a sharp corner. Let $\Omega = (-1,1)^2$. The interface is defined by the level-set function:

$$\Gamma(x,y) = -y^2 + ((x-1)\tan(\theta))^2 x, \quad \theta = 40. \tag{5.3}$$

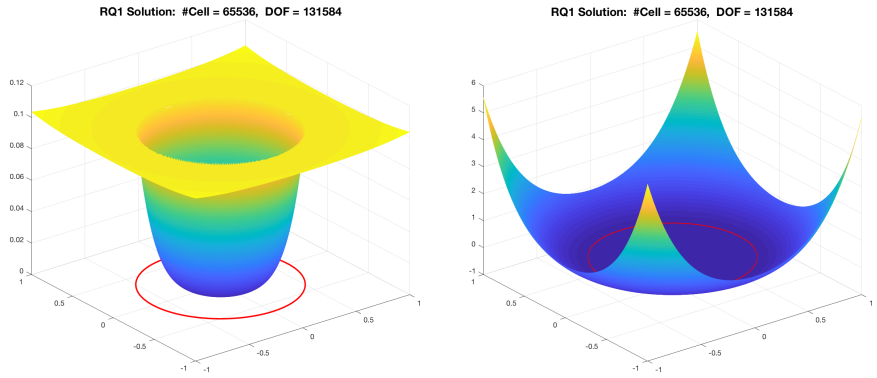

FIG. 5.1. *IFE solutions for Example 5.1 with* $(\beta^-, \beta+) = (1, 1000)$ *and* $(\beta^-, \beta+) = (1000, 1)$

TABLE 5.1
IFE solutions for the circular interface with $\beta^- = 1$, $\beta^+ = 1000$

N	DOF	$\|\cdot\|_{L^\infty}$	rate	$\|\cdot\|_{L^2}$	rate	$\|\cdot\|_{H^1}$	rate	Cond	rate
8	1.44E+2	$7.29E{-3}$		$1.05E{-2}$		$1.25E{-1}$		3.52E+4	
16	5.44E+2	$3.75E{-3}$	0.96	$3.96E{-3}$	1.41	$8.73E{-2}$	0.51	1.53E+5	-2.11
32	2.11E+3	$9.28E{-4}$	2.01	$9.43E{-4}$	2.06	$4.51E{-2}$	0.95	6.25E+5	-2.03
64	8.32E+3	$2.15E{-4}$	2.11	$2.31E{-4}$	2.03	$2.32E{-2}$	0.96	2.51E+6	-2.00
128	3.30E+4	$7.12E{-5}$	1.59	$5.85E{-5}$	1.98	$1.18E{-2}$	0.98	9.86E+6	-1.97
256	1.32E+5	$1.69E{-5}$	2.08	$1.44E{-5}$	2.02	$5.93E{-3}$	0.99	4.00E+7	-2.02
512	5.25E+5	$4.37E{-6}$	1.95	$3.62E{-6}$	1.99	$2.98E{-3}$	0.99	1.61E+8	-2.01
1024	2.10E+6	$1.14E{-6}$	1.94	$9.15E{-7}$	1.98	$1.49E{-3}$	1.00	6.46E+8	-2.00

TABLE 5.2
IFE solutions for the circular interface with $\beta^- = 1000$, $\beta^+ = 1$

N	DOF	$\|\cdot\|_{L^\infty}$	rate	$\|\cdot\|_{L^2}$	rate	$\|\cdot\|_{H^1}$	rate	Cond	rate
8	1.44E+2	$3.77E{-2}$		$1.42E{-1}$		$2.31E{-0}$		7.58E+4	
16	5.44E+2	$1.61E{-2}$	1.23	$3.63E{-2}$	1.97	$1.49E{-0}$	1.00	3.01E+5	-1.99
32	2.11E+3	$3.24E{-3}$	2.31	$9.05E{-3}$	2.00	$5.95E{-1}$	0.99	1.21E+6	-2.00
64	8.32E+3	$8.35E{-4}$	1.96	$2.27E{-3}$	2.00	$2.98E{-1}$	1.00	4.97E+6	-2.03
128	3.30E+4	$2.10E{-4}$	1.99	$5.68E{-4}$	2.00	$1.49E{-1}$	1.00	1.99E+7	-2.00
256	1.32E+5	$5.15E{-5}$	2.02	$1.42E{-4}$	2.00	$7.45E{-2}$	1.00	7.94E+7	-1.99
512	5.25E+5	$1.24E{-5}$	2.05	$3.55E{-5}$	2.00	$3.72E{-2}$	1.00	3.19E+8	-2.00
1024	2.10E+6	$3.17E{-6}$	1.97	$8.88E{-6}$	2.01	$1.86E{-2}$	1.00	1.27E+9	-2.00

The subdomains are defined as $\Omega^+ = \{(x, y) \in \Omega : \Gamma(x, y) > 0\}$, and $\Omega^- = \{(x, y) \in \Omega : \Gamma(x, y) < 0\}$. The exact solution is chosen as:

$$u(x,y) = \begin{cases} \dfrac{1}{\beta^-}\Gamma(x,y), & (x,y) \in \Omega^-, \\ \dfrac{1}{\beta^+}\Gamma(x,y), & (x,y) \in \Omega^+. \end{cases} \tag{5.4}$$

At the point $(1, 0)$, the interface curve has a sharp corner. The performance of our

numerical scheme is reported in Table 5.3 and Table 5.4 for he high coefficient jump cases $(\beta^-, \beta^+) = (1, 1000)$ and $(\beta^-, \beta^+) = (1000, 1)$, respectively. Similar conclusions as previous ones can be made for such convergence tests. Furthermore, the numerical solutions are plotted in Figure 5.2.

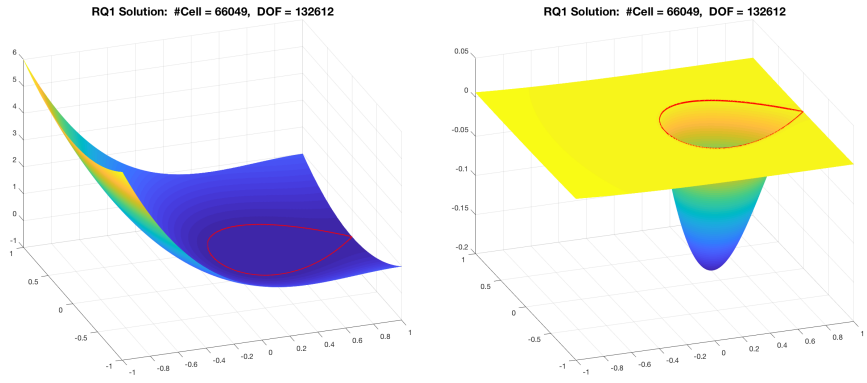

FIG. 5.2. *IFE solutions for Example 5.2 with* $(\beta^-, \beta+) = (1, 1000)$ *and* $(\beta^-, \beta+) = (1000, 1)$

TABLE 5.3
IFE solutions for sharp-corner interface with $\beta^- = 1$, $\beta^+ = 1000$

N	DOF	$\|\cdot\|_{L^\infty}$	rate	$\|\cdot\|_{L^2}$	rate	$\|\cdot\|_{H^1}$	rate	Cond	rate
8	1.44E+2	$1.91E{-}2$		$4.02E{-}2$		$8.25E{-}1$		6.83E+4	
16	5.44E+2	$6.04E{-}3$	1.66	$1.00E{-}2$	2.00	$4.12E{-}1$	1.00	2.62E+5	-1.94
32	2.12E+3	$1.74E{-}3$	1.79	$2.59E{-}3$	1.95	$2.06E{-}1$	1.00	1.01E+6	-1.95
64	8.32E+3	$4.50E{-}4$	1.95	$6.66E{-}4$	1.96	$1.03E{-}1$	0.99	3.99E+6	-1.98
128	3.30E+4	$1.22E{-}4$	1.88	$1.66E{-}4$	2.01	$5.14E{-}2$	1.00	1.58E+7	-1.98
256	1.32E+5	$4.02E{-}5$	1.61	$4.12E{-}5$	2.00	$2.57E{-}2$	1.00	6.24E+7	-1.98
512	5.25E+5	$1.14E{-}5$	1.82	$1.03E{-}5$	2.00	$1.29E{-}2$	1.00	2.47E+8	-1.99
1024	2.10E+6	$2.86E{-}6$	1.99	$2.58E{-}6$	2.00	$6.43E{-}3$	1.00	9.81E+8	-1.99

TABLE 5.4
IFE solutions for sharp-corner interface with $\beta^- = 1000$, $\beta^+ = 1$

N	DOF	$\|\cdot\|_{L^\infty}$	rate	$\|\cdot\|_{L^2}$	rate	$\|\cdot\|_{H^1}$	rate	Cond	rate
8	1.44E+2	$3.45E{-}2$		$1.70E{-}2$		$1.62E{-}1$		1.70E+4	
16	5.44E+2	$9.29E{-}3$	1.89	$4.10E{-}3$	2.05	$8.38E{-}2$	0.95	7.08E+4	-2.06
32	2.11E+3	$2.28E{-}3$	2.03	$1.00E{-}3$	2.03	$4.18E{-}2$	1.00	2.91E+5	-2.04
64	8.32E+3	$5.24E{-}4$	2.12	$2.57E{-}4$	1.96	$2.07E{-}2$	1.01	1.16E+6	-1.99
128	3.30E+4	$1.33E{-}4$	1.98	$6.22E{-}5$	2.05	$1.03E{-}2$	1.01	4.66E+6	-2.01
256	1.32E+5	$3.08E{-}5$	2.11	$1.49E{-}5$	2.06	$5.14E{-}3$	1.01	1.88E+7	-2.01
512	5.25E+5	$9.54E{-}6$	1.69	$3.70E{-}6$	2.01	$2.56E{-}3$	1.01	7.52E+7	-2.00
1024	2.10E+6	$2.38E{-}6$	2.00	$9.28E{-}7$	2.00	$1.28E{-}3$	1.00	3.01E+8	-2.00

5.3. Comparison with Lagrangian IFE Methods. In this subsection, we address some similarities and differences between the nonconforming Q_1-IFE method

and the conforming Q_1-IFE method discussed in [16, 18, 26].

Both IFE methods can solve the interface problem (1.1)-(1.3) on rectangular Cartesian meshes. In terms of computational cost, the conforming IFE method is cheaper because the degrees of freedom of the nonconforming IFE method are about twice as much as that of the conforming IFE method on the same mesh of $N \times N$ rectangles. However, the nonconforming IFE method is advantageous in term of accuracy and convergence. In Figure 5.3, we use the error surfaces to compare the accuracy of these two IFE methods for the circular interface problem in Section 5.1 on the same mesh containing 80×80 cells. We notice that the error of conforming IFE solution is much larger around interface than the rest of domain such that its error surface possesses a prominent "interface error crown". In contrast, not only the nonconforming IFE solution is much more accurate than the conforming IFE solution around the interface, but also its accuracy around interface is comparable to the accuracy in areas away from the interface. Also as discussed in [28], the convergence order in H^1- and L^2- norms for conforming IFE method can sometimes deteriorate as the mesh size becomes small, and the order in L^∞-norm can become far from the second order. Adding penalty terms can eliminate these shortcomings of the conforming IFE method [28], but this leads to a more complicated IFE method with a higher computational cost while the nonconforming Q_1-IFE method is based on the simple Galerkin formulation and still converges optimally.

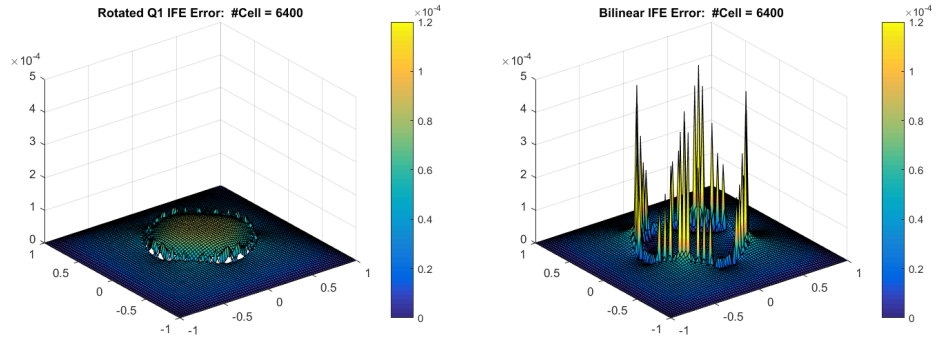

FIG. 5.3. *Error surfaces of the nonconforming and conforming Q_1-IFE solutions*

We compare the discontinuity in a global basis of the conforming Q_1-IFE space with its counterpart in the nonconforming Q_1-IFE space defined on the same mesh. The first two plots from the left in Figure 5.4 are for the conforming Q_1 basis and the corresponding nonconforming Q_1-IFE basis over two typical interface elements, respectively. An obviously large gap along the interface edge in the first plot of Figure 5.4 shows a much stronger discontinuity of the conforming Q_1-IFE basis than the corresponding nonconforming Q_1-IFE basis shown in the second plot of Figure 5.4. Furthermore, we plot the traces of these IFE bases on an interface edge in the right plot of Figure 5.4. The blue curves in this plot are for the conforming Q_1-IFE basis which are far more apart than the red trace curves for the nonconforming-Q_1-IFE basis. From this plot, we can see the fact that, over each interface edge, the continuity of a conforming Q_1-IFE basis is only maintained at the two end points, but the continuity of a nonconforming Q_1-IFE basis is maintained over the whole interface edge. It is our belief that the less discontinuity in the nonconforming Q_1-IFE functions is a key factor for the advantages of the nonconforming Q_1-IFE method.

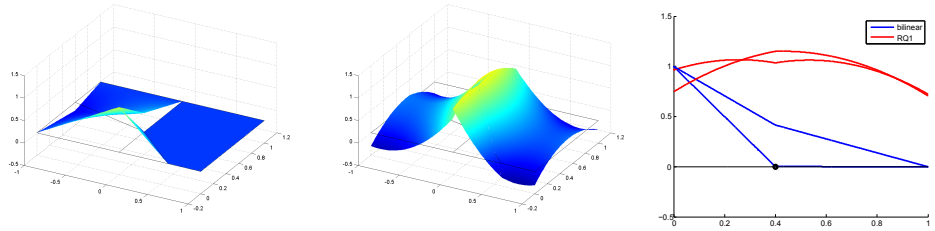

FIG. 5.4. *Conforming Q_1-IFE and nonconforming Q_1-IFE bases with $\beta^- = 1$, $\beta^+ = 1000$.*

6. Conclusions. In this article, we develop the nonconforming Q_1-IFE space based on mean-value degrees of freedom. The new nonconforming IFE method is based on the standard Galerkin formulation. Error analysis shows the quasi-optimal convergence in both energy and the L^2-norms.

REFERENCES

[1] I. Babuška. The finite element method for elliptic equations with discontinuous coefficients. *Computing (Arch. Elektron. Rechnen)*, 5:207–213, 1970.

[2] D. Boffi, F. Brezzi and M. Fortin. *Mixed finite element methods and applications*. Springer, Heidelberg, 2013. Springer Series in Computational Mathematics, 44.

[3] W. Cao, X. Zhang, and Z. Zhang. Superconvergence of immersed finite element methods for interface problems. *Adv. Comput. Math.*, 43(4):795–821, 2017.

[4] Z. Chen and P. Oswald. Multigrid and multilevel methods for nonconforming Q_1 elements. *Math. Comp.*, 67(222):667–693, 1998.

[5] Z. Chen and J. Zou. Finite element methods and their convergence for elliptic and parabolic interface problems. *Numer. Math.*, 79(2):175–202, 1998.

[6] P. G. Ciarlet. *The finite element method for elliptic problems*. North-Holland Publishing Co., Amsterdam-New York-Oxford, 1978. Studies in Mathematics and its Applications, Vol. 4.

[7] M. Crouzeix and P.-A. Raviart. Conforming and nonconforming finite element methods for solving the stationary Stokes equations. I. *Rev. Française Automat. Informat. Recherche Opérationnelle Sér. Rouge*, 7(R-3):33–75, 1973.

[8] J. Douglas, Jr., J. E. Santos, D. Sheen, and X. Ye. Nonconforming Galerkin methods based on quadrilateral elements for second order elliptic problems. *M2AN Math. Model. Numer. Anal.*, 33(4):747–770, 1999.

[9] V. Girault and P.-A. Raviart. *Finite element methods for Navier-Stokes equations*, volume 5 of *Springer Series in Computational Mathematics*. Springer-Verlag, Berlin, 1986. Theory and algorithms.

[10] Y. Gong, B. Li, and Z. Li. Immersed-interface finite-element methods for elliptic interface problems with nonhomogeneous jump conditions. *SIAM J. Numer. Anal.*, 46(1):472–495, 2007/08.

[11] R. Guo and T. Lin. A group of immersed finite element spaces for elliptic interface problems. *IMA J. Numer. Anal.*, 2017. DOI: 10.1093/imanum/drx074.

[12] R. Guo, T. Lin, and X. Zhang. Nonconforming Immersed Finite Element Spaces for Elliptic Interface Problems. *Comput. Math. Appl.*, 75(6):2002–2016, 2018.

[13] J. Guzmán, M. A. Sánchez, and M. Sarkis. Higher-order finite element methods for elliptic problems with interfaces. *ESAIM Math. Model. Numer. Anal.*, 50(5):1561–1583, 2016.

[14] J. Guzmán, M. A. Sánchez, and M. Sarkis. On the accuracy of finite element approximations to a class of interface problems. *Math. Comp.*, 85(301):2071–2098, 2016.

[15] J. Guzmán, M. A. Sánchez, and M. Sarkis. A finite element method for high-contrast interface problems with error estimates independent of contrast. *J. Sci. Comput.*, 73(1):330–365, 2017.

[16] X. He, T. Lin, and Y. Lin. Approximation capability of a bilinear immersed finite element space. *Numer. Methods Partial Differential Equations*, 24(5):1265–1300, 2008.

[17] X. He, T. Lin, and Y. Lin. Immersed finite element methods for elliptic interface problems with non-homogeneous jump conditions. *Int. J. Numer. Anal. Model.*, (2):284-301, 2011.

[18] X. He, T. Lin, and Y. Lin. The convergence of the bilinear and linear immersed finite element solutions to interface problems. *Numer. Methods Partial Differential Equations*, 28(1):312–330, 2012.

[19] X. He, T. Lin, Y. Lin, and X. Zhang. Immersed finite element methods for parabolic equations with moving interface. *Numer. Methods Partial Differential Equations*, 29(2):619–646, 2013.

[20] H. Ji, J. Chen, and Z. Li. A symmetric and consistent immersed finite element method for interface problems. *J. Sci. Comput.*, 61(3):533–557, 2014.

[21] R. Kafafy, T. Lin, Y. Lin, and J. Wang. Three-dimensional immersed finite element methods for electric field simulation in composite materials. *Internat. J. Numer. Methods Engrg.*, 64(7):940–972, 2005.

[22] R. Kafafy and J. Wang. Whole ion optics gridlet simulations using a hybrid-grid immersed-finite-element particle-in-cell code. *J. Propulsion Power*, 23(1):59–68, 2007.

[23] P. Klouček, B. Li, and M. Luskin. Analysis of a class of nonconforming finite elements for crystalline microstructures. *Math. Comp.*, 65(215):1111–1135, 1996.

[24] Z. Li, T. Lin, Y. Lin, and R. C. Rogers. An immersed finite element space and its approximation capability. *Numer. Methods Partial Differential Equations*, 20(3):338–367, 2004.

[25] Z. Li, T. Lin, and X. Wu. New Cartesian grid methods for interface problems using the finite element formulation. *Numer. Math.*, 96(1):61–98, 2003.

[26] T. Lin, Y. Lin, R. Rogers, and M. L. Ryan. A rectangular immersed finite element space for interface problems. In *Scientific computing and applications (Kananaskis, AB, 2000)*, volume 7 of *Adv. Comput. Theory Pract.*, pages 107–114. Nova Sci. Publ., Huntington, NY, 2001.

[27] T. Lin, Y. Lin, and X. Zhang. A method of lines based on immersed finite elements for parabolic moving interface problems. *Adv. Appl. Math. Mech.*, 5(4):548–568, 2013.

[28] T. Lin, Y. Lin, and X. Zhang. Partially penalized immersed finite element methods for elliptic interface problems. *SIAM J. Numer. Anal.*, 53(2):1121–1144, 2015.

[29] T. Lin, D. Sheen, and X. Zhang. A locking-free immersed finite element method for planar elasticity interface problems. *J. Comput. Phys.*, 247:228–247, 2013.

[30] T. Lin, Q. Yang, and X. Zhang. *A Priori* error estimates for some discontinuous Galerkin immersed finite element methods. *J. Sci. Comput.*, 65(3):875–894, 2015.

[31] R. Rannacher and S. Turek. Simple nonconforming quadrilateral Stokes element. *Numer. Methods Partial Differential Equations*, 8(2):97–111, 1992.

[32] S. Vallaghé and T. Papadopoulo. A trilinear immersed finite element method for solving the electroencephalography forward problem. *SIAM J. Sci. Comput.*, 32(4):2379–2394, 2010.

[33] X. Zhang. *Nonconforming Immersed Finite Element Methods for Interface Problems*. 2013. Thesis (Ph.D.)–Virginia Polytechnic Institute and State University.